The Astrophysical Journal Letters, 899:L23 (7pp), 2020 August 20 https://doi.org/10.3847/2041-8213/abab0c
© 2020. The Author(s). Published by the American Astronomical Society.
OPEN ACCESS

Destruction of Molecular Hydrogen Ice and Implications for 1I/2017 U1 ('Oumuamua)

Thiem Hoang[1,2] and Abraham Loeb[3]
[1] Korea Astronomy and Space Science Institute, Daejeon 34055, Republic of Korea; thiemhoang@kasi.re.kr
[2] Korea University of Science and Technology, Daejeon 34113, Republic of Korea
[3] Astronomy Department, Harvard University, 60 Garden Street, Cambridge, MA, USA; aloeb@cfa.harvard.edu
Received 2020 June 14; revised 2020 July 13; accepted 2020 July 31; published 2020 August 17

Abstract

The first interstellar object observed in our solar system, 1I/2017 U1 ('Oumuamua), exhibited a number of peculiar properties, including extreme elongation and acceleration excess. Recently, Seligman & Laughlin proposed that the object was made out of molecular hydrogen (H_2) ice. The question is whether H_2 objects could survive their travel from the birth sites to the solar system. Here we study destruction processes of icy H_2 objects through their journey from giant molecular clouds (GMCs) to the interstellar medium (ISM) and the solar system, owing to interstellar radiation, gas and dust, and cosmic rays. We find that thermal sublimation due to heating by starlight can destroy 'Oumuamua-size objects in less than 10 Myr. Thermal sublimation by collisional heating in GMCs could destroy H_2 objects of 'Oumuamua-size before their escape into the ISM. Most importantly, the formation of icy grains rich in H_2 is unlikely to occur in dense environments because collisional heating raises the temperature of the icy grains, so that thermal sublimation rapidly destroys the H_2 mantle before grain growth.

Unified Astronomy Thesaurus concepts: A stars (5); Amor group (36); Interstellar dynamics (839); Dense interstellar clouds (371); Astrosphere interstellar medium interactions (106); Comets (280); Aperiodic comets (52); Asteroids (72)

1. Introduction

The detection of the first interstellar object, 1I/2017 U1 ('Oumuamua) by the Pan-STARRS survey (Bacci et al. 2017) implies an abundant population of similar interstellar objects (Meech et al. 2017; Do et al. 2018). An elongated shape of semi-axes $\sim 230\,\mathrm{m} \times 35\,\mathrm{m}$ is estimated from light-curve modeling (Jewitt et al. 2017). The extreme axial ratio of $\gtrsim 5:1$ implied by 'Oumuamua's light curve is mysterious (Gaidos et al. 2017; Fraser et al. 2018).

Bannister et al. (2017) and Gaidos (2017) suggested that 'Oumuamua is a contact binary, while others speculated that the bizarre shape might be the result of violent processes, such as collisions during planet formation. Domokos et al. (2017) suggested that the elongated shape might arise from ablation induced by interstellar dust, and Hoang et al. (2018) suggested that it could originate from rotational disruption of the original body by mechanical torques. Sugiura et al. (2019) suggested that the extreme elongation might arise from planetesimal collisions. The latest proposal involved tidal disruption of a larger parent object close to a dwarf star (Zhang & Lin 1919), but this mechanism is challenged by the preference for a disk-like shape implied by 'Oumuamua's light curve (Mashchenko 2019).

Another peculiarity is the detection of non-gravitational acceleration in the trajectory of 'Oumuamua (Micheli et al. 2018). The authors suggested that cometary activity such as outgassing of volatiles could explain the acceleration excess. Interestingly, no cometary activity of carbon-based molecules was found by deep observations with the Spitzer space telescope (Trilling et al. 2018) and Gemini North telescope (Drahus et al. 2018). Bialy & Loeb (2018) explained the acceleration anomaly by means of radiation pressure acting on a thin lightsail, and Moro-Martin (2019) and Sekanina (2019) suggested a porous object. Fitzsimmons et al. (2018) proposed that an icy object of unusual composition might survive its interstellar journey. Previously, Füglistaler & Pfenniger (2018) suggested that 'Oumuamua might be composed of H_2. However, Rafikov (2018) argued that the level of outgassing needed to produce the acceleration excess would rapidly change the rotation period of 'Oumuamua, in conflict with the observational data.

Most recently, Seligman & Laughlin (2020) suggested hydrogen ice to explain 'Oumuamua's excess acceleration and unusual shape. Their modeling implied that the object is ~ 100 Myr old. Assuming a speed of $30\,\mathrm{km\,s^{-1}}$, they suggested that the object was produced in a giant molecular cloud (GMC) at a distance of ~ 5 kpc. However, their study did not consider the destruction of H_2 ice in the interstellar medium (ISM), but only through evaporation by sunlight. Here, we explore the evolution of H_2 ices from their potential GMC birth sites to the diffuse ISM and eventually the solar system.

Assuming that H_2 objects could be formed in GMCs by some mechanisms (Füglistaler & Pfenniger 2016; Füglistaler & Pfenniger 2018; Seligman & Laughlin 2020), we quantify their destruction and determine the minimum size of an H_2 object that can reach the solar system. We assume that the H_2 objects are ejected from GMCs into the ISM by some dynamical mechanism such as tidal disruption of bigger objects or collisions (see Raymond et al. 2018; Rice & Laughlin 2019). The evolution of H_2 objects in the ISM has additional implications for baryonic dark matter (White 1996; Carr & Sakellariadou 1999).

The structure of this Letter is as follows. In Sections 2–4, we calculate the destruction timescales from various processes for H_2 objects. In Section 5, we compare the destruction times with the travel time for different object sizes. In Section 6, we explore the formation of H_2-rich objects in dense GMCs and

Original content from this work may be used under the terms of the Creative Commons Attribution 4.0 licence. Any further distribution of this work must maintain attribution to the author(s) and the title of the work, journal citation and DOI.

the implications for baryonic dark matter. We conclude with a summary of our main findings in Section 7.

2. Destruction of H_2 Ice by Interstellar Radiation

Let us first assume that H_2 objects could form in dense GMCs and get ejected into the ISM and examine several mechanisms for H_2 ice destruction. The binding energy of H_2 in the hydrogen ice is $E_b/k \sim 100$ K (Sandford & Allamandola 1993), equivalent to $E_b(H_2) \approx 0.01$ eV . For simplicity, we assume a spherical object shape in our derivations, but the results can be easily generalized to other shapes.

2.1. Thermal Sublimation

Heating by starlight and cosmic microwave background (CMB) radiation raises the surface temperature of H_2 ice. We assume that the local interstellar radiation field (ISRF) has the same spectrum as the ISRF in the solar neighborhood (Mathis et al. 1983) with a total radiation energy density of $u_{\rm MMP} \approx 8.64 \times 10^{-13}$ erg cm^{-3}. We calibrate the strength of the local radiation field by the dimensionless parameter, U, so that the local energy density is $u_{\rm rad} = Uu_{\rm MMP}$. The CMB radiation is blackbody with a temperature $T_{\rm CMB} = 2.725(1+z)$ K at a redshift z, and the radiation energy density is $u_{\rm CMB} = \int 4\pi B_\nu(T_{\rm CMB})\ d\nu/c = 4\sigma T_{\rm CMB}^4/c \approx 4.17 \times 10^{-13}(1+z)^4$ erg cm^{-3}. At present, heating by the CMB is less important than by starlight.

The characteristic timescale for the evaporation of an H_2 molecule from a surface of temperature $T_{\rm ice}$ is

$$\tau_{\rm sub} = \nu_0^{-1} \exp\left(\frac{E_b}{kT_{\rm ice}}\right), \tag{1}$$

where ν_0 is the characteristic oscillation frequency of the H_2 lattice (Watson & Salpeter 1972). We adopt $\nu_0 = 10^{12}$ s^{-1} for H_2 ice (Hegyi & Olive 1986; Sandford & Allamandola 1993).

Assuming that the H_2 ice has a layered structure, the sublimation rate for an H_2 object of radius R is given by

$$\frac{dR}{dt} = -\frac{\nu_0}{n_{\rm ice}^{1/3}} \exp\left(-\frac{E_b}{kT_{\rm ice}}\right), \tag{2}$$

where $n_{\rm ice} \approx 3 \times 10^{22}$ cm^{-3} is the molecular number density of H_2 ice with a mass density of $\rho_{\rm ice} = 0.1$ g cm^{-3}.

The sublimation time is then

$$t_{\rm sub}(T_{\rm ice}) = -\frac{R}{dR/dt} = \frac{Rn_{\rm ice}^{1/3}}{\nu_0} \exp\left(\frac{E_b}{kT_{\rm ice}}\right), \tag{3}$$

where dR/dt was substituted from Equation (2).

Plugging the numerical parameters into the above equation, we obtain

$$t_{\rm sub}(T_{\rm ice}) \simeq 2.95 \times 10^7 \left(\frac{R}{1\ {\rm km}}\right) \times \exp\left(100\ {\rm K}\left[\frac{1}{T_{\rm ice}} - \frac{1}{3\ {\rm K}}\right]\right) {\rm yr} \tag{4}$$

for H_2 ice, and the ice temperature is normalized to $T_{\rm ice} = 3$ K expecting that starlight raises the surface temperature above $T_{\rm CMB}$. At the minimum temperature of the present-day CMB radiation, $T_{\rm obj} = 2.725$ K, the sublimation time is $t_{\rm sub} \approx 0.85$ Gyr for $R = 1$ km.

The heating rate due to absorption of isotropic interstellar radiation and CMB photons is given by

$$\frac{dE_{\rm abs}}{dt} = \pi R^2 c(Uu_{\rm MMP} + u_{\rm CMB})\epsilon_\star, \tag{5}$$

where $\epsilon_\star$ is the surface emissivity averaged over the background radiation spectrum.

The cooling rate by thermal emission is given by

$$\frac{dE_{\rm emiss}}{dt} = 4\pi R^2 \epsilon_T \sigma T^4, \tag{6}$$

where $\epsilon_T = \int d\nu \epsilon(\nu) B_\nu(T) \big/ \int d\nu B_\nu(T)$ is the bolometric emissivity, integrated over all radiation frequencies, ν.

The energy balance between radiative heating and cooling yields the surface equilibrium temperature

$$T_{\rm ice} = \left(\frac{c(Uu_{\rm MMP} + u_{\rm CMB})}{4\sigma}\right)^{1/4} \left(\frac{\epsilon_\star}{\epsilon_T}\right)^{1/4} \simeq 3.59(U + [1+z]^3)^{1/4} \left(\frac{\epsilon_\star}{\epsilon_T}\right)^{1/4} {\rm K}. \tag{7}$$

At this temperature, the sublimation time is short, less than $\sim 1 \times 10^5$ yr, according to Equation (4).

However, to access the actual temperature of the ice, we need to take account of evaporative cooling (Watson & Salpeter 1972; Hoang et al. 2015). The cooling rate by evaporation of H_2 is given by

$$\frac{dE_{\rm evap}}{dt} = \frac{E_b dN_{\rm mol}}{dt} = \frac{E_b N_s}{\tau_{\rm sub}(T_{\rm ice})}, \tag{8}$$

where $dN_{\rm mol}/dt$ is the evaporation rate, namely, the number of molecules evaporating per unit time, and $N_s = 4\pi R^2/r_s^2$ is the number of surface sites with $r_s = 10$ Å being the average size of the H_2 surface site (Sandford & Allamandola 1993).

The ratio of evaporative to radiative cooling rates is given by

$$\frac{dE_{\rm evap}/dt}{dE_{\rm emiss}/dt} = \frac{E_b \nu_0 \exp(-E_b/kT_{\rm ice})}{\epsilon_T \sigma T_{\rm ice}^4 r_s^2} \simeq \left(\frac{1.1}{\epsilon_T}\right)\left(\frac{3\ {\rm K}}{T_{\rm ice}}\right)^4 \exp\left(100\ {\rm K}\left[\frac{1}{T_{\rm ice}} - \frac{1}{3\ {\rm K}}\right]\right) \times \left(\frac{E_b}{0.01\ {\rm eV}}\right)\left(\frac{10\ \text{Å}}{r_s}\right)^2, \tag{9}$$

implying that the evaporative cooling dominates over radiative cooling for $T_{\rm ice} \gtrsim 3$ K.

For an H_2 object moving at a speed, $v_{\rm obj}$, through the ISM, the heating rate by gas collisions is given by

$$\frac{dE_{\rm coll}}{dt} = \frac{1}{2}\pi R^2 n_{\rm H} \mu m_{\rm H} v_{\rm obj}^3, \tag{10}$$

where μ is the mean molecular weight of the ISM and $m_{\rm H}$ is the mass of a hydrogen atom. For the cosmic He abundance, $\mu = 1.4$.

The ratio of collisional heating to radiative heating by starlight is given by

$$\frac{dE_{\rm coll}}{dE_{\rm abs}} = \frac{(n_{\rm H}\mu m_{\rm H} v_{\rm obj}^3/2)}{cUu_{\rm MMP}\epsilon_\star} \simeq 1.2\left(\frac{n_{\rm H}}{10^3\,{\rm cm}^{-3}}\right)\left(\frac{v_{\rm obj}}{30\,{\rm km\,s}^{-1}}\right)^3\left(\frac{U}{\epsilon_\star}\right), \quad (11)$$

implying dominance of collisional heating if $n_{\rm H} \gtrsim cUu_{\rm MMP}/(\mu m_{\rm H} v_{\rm obj}^3/2) \simeq 825U\,(30\,{\rm km\,s}^{-1}/v_{\rm obj})^3\,{\rm cm}^{-3}$, assuming $\epsilon_\star = 1$. Thus, in GMCs, collisional heating is important and can destroy H_2 objects rapidly (see Section 5). For the diffuse ISM, collisional heating is negligible.

The final energy balance equation reads

$$\frac{dE_{\rm abs}}{dt} + \frac{dE_{\rm coll}}{dt} = \frac{dE_{\rm emiss}}{dt} + \frac{dE_{\rm evap}}{dt}. \quad (12)$$

We numerically solve the above equation for the equilibrium temperature, and obtain $T_{\rm ice} = 2.996 \approx 3$ K, assuming $U = 1$, the present CMB, and $n_{\rm H} = 10\,{\rm cm}^{-3}$. At this temperature, Equation (4) implies the sublimation time of ~30 Myr for $R = 1$ km. Passing near a region with enhanced radiation fields, e.g., near a star, would reduce the sublimation time significantly.

2.2. Photodesorption

Next we estimate the lifetime of an icy H_2 object to ultraviolet (UV) photodesorption. Let $Y_{\rm pd}$ be the photodesorption yield, defined as the number of molecules ejected over the total number of incident UV photons. The rate of mass loss due to UV photodesorption is

$$\frac{dm}{dt} = \frac{4\pi R^2 \rho_{\rm ice} dR}{dt} = -\bar{m} Y_{\rm pd} F_{\rm UV} \pi a^2, \quad (13)$$

where $\bar{m}$ is the mean mass of ejected molecules, and $F_{\rm UV}$ is the flux of UV photons. This yields

$$\frac{dR}{dt} = -\frac{\bar{m} Y_{\rm pd} F_{\rm UV}}{4\rho_{\rm ice}} \simeq -262\left(\frac{F_{\rm UV}}{10^7\,{\rm cm}^{-2}\,{\rm s}^{-1}}\right)\left(\frac{Y_{\rm pd}}{10^3}\right)\left(\frac{0.1\,{\rm g\,cm}^{-3}}{\rho_{\rm ice}}\right)\,{\rm \AA\ yr}^{-1}, \quad (14)$$

where $\bar{m} = 2m_{\rm H}$, $Y_{\rm pd} = h\nu/E_b = 10^3$ for $h\nu = 10$ eV, and $F_{\rm UV} = 10^7\,{\rm cm}^{-2}\,{\rm s}^{-1}$ for the ISRF.

We define $G = F_{\rm UV}/F_{\rm UV,MMP}$ to calibrate the strength of background UV radiation, where $F_{\rm UV,MMP} = 10^7\,{\rm cm}^{-2}\,{\rm s}^{-1}$ is the UV flux of the standard ISRF. The photodesorption time for an object of radius R is

$$t_{\rm pd} = -\frac{R}{dR/dt} \simeq \frac{7.5\times10^{10}}{G}\left(\frac{R}{1\,{\rm km}}\right)\left(\frac{10^3}{Y_{\rm pd}}\right)\left(\frac{10^7\,{\rm cm}^{-2}\,{\rm s}^{-1}}{F_{\rm UV,MMP}}\right){\rm yr}. \quad (15)$$

An enhancement of the local UV radiation near an OB association can increase the photodesorption rate by a factor of G.

3. Destruction by Cosmic Rays

The stopping power of a relativistic proton in H_2 ice is $dE/dx \sim -10^6$ eV cm^{-1} at an energy $E \sim 1$ GeV (Hoang et al. 2015; Hoang et al. 2017). The corresponding penetration length is $R_p = -E/(dE/dx) \sim 10^3$ cm = 10 m.

The ice volume evaporated by a cosmic ray (CR) proton is determined by the heat transfer from the CR to the ice volume that reaches an evaporation temperature $T_{\rm evap} \sim E_b/3k$ (i.e., thermal energy per H_2 comparable to the binding energy). Because the object radius is much larger than the above penetration length, the volume of ice evaporated by a CR proton, δV, is given by

$$n_{\rm ice}\delta V E_b = E_{\rm CR}. \quad (16)$$

Because the penetration length is much shorter than the 'Oumuamua's estimated size, CRs would gradually erode the object. The fraction of the object volume eroded by CRs per unit of time is

$$\frac{1}{V}\frac{dV}{dt} = -\frac{4\pi R^2 F_{\rm CR}\delta V}{V} = -\frac{3F_{\rm CR}E_{\rm CR}}{Rn_{\rm ice}E_b}, \quad (17)$$

where $V = 4\pi R^3/3$ is the object's volume.

The timescale required to eliminate the object is

$$t_{\rm CR} = -\frac{V}{dV/dt} = \frac{Rn_{\rm ice}E_b}{3F_{\rm CR}E_{\rm CR}} \simeq 3.2\times10^8\left(\frac{R}{1\,{\rm km}}\right)\left(\frac{E_b}{0.01\,{\rm eV}}\right)\left(\frac{10^9\,{\rm eV}}{E_{\rm CR}}\right) \times\left(\frac{1\,{\rm cm}^{-2}\,{\rm s}^{-1}}{F_{\rm CR}}\right){\rm yr}, \quad (18)$$

where $F_{\rm CR} = 1\,{\rm cm}^{-2}\,{\rm s}^{-1}$ is the flux of proton CRs of $E = 1$ GeV. The above result is comparable to the estimate by White (1996).

The contribution of heavy-ion CRs is less important than proton CRs because their flux is lower; for iron ions, the abundance ratio is $F_{\rm Fe}/F_p = 1.63\times10^{-4}$ (see Leger et al. 1985).

4. Destruction by Interstellar Matter

4.1. Nonthermal Sputtering

At a characteristic speed of $v_{\rm obj} \sim 30\,{\rm km\,s}^{-1}$, each ISM proton delivers an energy of $E_p = m_{\rm H}v_{\rm obj}^2/2 \approx 4.66$ eV to the impact location. Thus, protons can eject H_2 out of the ice surface with a sputtering yield of $Y_{\rm sp} \sim E_p/E_b \sim 460$.

The destruction time of H_2 ice by sputtering is given by

$$t_{\rm sp} = -\frac{R}{dR/dt} = \frac{4\rho_{\rm ice}R}{n_{\rm H}m_{\rm H}v_{\rm obj}Y_{\rm sp}} \simeq 2.6\times10^{10}\left(\frac{0.1\,{\rm g\,cm}^{-3}}{\rho_{\rm ice}}\right)\left(\frac{R}{1\,{\rm km}}\right)\left(\frac{10\,{\rm cm}^{-3}}{n_{\rm H}}\right) \times\left(\frac{30\,{\rm km\,s}^{-1}}{v_{\rm obj}}\right)\left(\frac{10^3}{Y_{\rm sp}}\right){\rm yr}, \quad (19)$$

which is short only in GMCs and unimportant for the diffuse ISM. Moreover, most of proton's energy may go into forming a deep track instead of surface heating, reducing the sputtering effect.

4.2. Impulsive Collisional Heating and Transient Evaporation

Collisions of H_2 ice with the ambient gas at high speeds can heat the frontal area to a temperature $T_{\rm evap}$, resulting in transient evaporation. The volume of ice evaporated by a single collision, δV, can be given by

$$n_{\rm ice}\delta V E_b = \frac{1}{2}\mu m_{\rm H} v_{\rm obj}^2, \tag{20}$$

where the impact kinetic energy is assumed to to be fully converted into heating.

The evaporation rate by gas collisions is given by

$$\frac{1}{V}\frac{dV}{dt} = -\frac{\pi R^2 n_{\rm H} v_{\rm obj}\delta V}{V} = -\frac{3 n_{\rm H}\mu m_{\rm H} v_{\rm obj}^3}{8 R n_{\rm ice} E_b}. \tag{21}$$

The evaporation time by gas collisions is then

$$\begin{aligned} t_{\rm evap,gas} &= -\frac{V}{dV/dt} = \frac{8 R n_{\rm ice} E_b}{3 n_{\rm H}\mu m_{\rm H} v^3} \\ &\simeq 6.5\times 10^9\left(\frac{R}{1\ {\rm km}}\right)\left(\frac{30\ {\rm km\ s^{-1}}}{v_{\rm obj}}\right)^3 \\ &\times\left(\frac{n_{\rm H}}{10\ {\rm cm^{-3}}}\right)^{-1}\left(\frac{E_b}{0.01\ {\rm eV}}\right){\rm yr}, \end{aligned} \tag{22}$$

which is somewhat shorter than the sputtering time given in Equation (19).

Similarly, dust grains of mass m_{gr} deposit a kinetic energy of $E_{\rm gr} = m_{\rm gr} v_{\rm obj}^2/2$ upon impact, resulting in transient evaporation. The evaporation rate by dust collisions is given by

$$\frac{1}{V}\frac{dV}{dt} = -\frac{\pi R^2 n_{\rm gr} v_{\rm obj}\delta V}{V} = -\frac{3 n_{\rm gr} m_{\rm gr} v_{\rm obj}^3}{8 R n_{\rm ice} E_b}, \tag{23}$$

yielding a dust evaporation time,

$$t_{\rm evap,d} = -\frac{V}{dV/dt} = \frac{8 R n_{\rm ice} E_b}{3 n_{\rm gr} m_{\rm gr} v_{\rm obj}^3}. \tag{24}$$

Assuming that all grains have the same size, a, and using the dust-to-gas mass ratio $M_{d/g} = n_{\rm gr} 4\pi a^3 \rho_{\rm gr}/(3\mu m_{\rm H} n_{\rm H})$, one obtains the grain number density

$$\begin{aligned} n_{\rm gr} &= \frac{M_{d/g}(3\mu m_{\rm H} n_{\rm H})}{4\pi a^3 \rho_{\rm gr}} \\ &\approx 1.85\times 10^{-11}\left(\frac{M_{d/g}}{100}\right)\left(\frac{n_{\rm H}}{10\ {\rm cm^{-3}}}\right) \\ &\times\left(\frac{0.1\ \mu{\rm m}}{a}\right)^3 {\rm cm^{-3}}, \end{aligned} \tag{25}$$

where $\rho_{\rm gr} = 3\ {\rm g\ cm^{-3}}$ is assumed.

Substituting $n_{\rm gr}$ into Equation (24) yields

$$\begin{aligned} t_{\rm evap,d} &\simeq 6.5\times 10^{11}\left(\frac{R}{1\ {\rm km}}\right)\left(\frac{30\ {\rm km\ s^{-1}}}{v_{\rm obj}}\right)^3 \\ &\times\left(\frac{n_{\rm H}}{10\ {\rm cm^{-3}}}\right)\left(\frac{E_b}{0.01\ {\rm eV}}\right){\rm yr}. \end{aligned} \tag{26}$$

The destruction by dust is less efficient than by gas due to a lower dust mass.

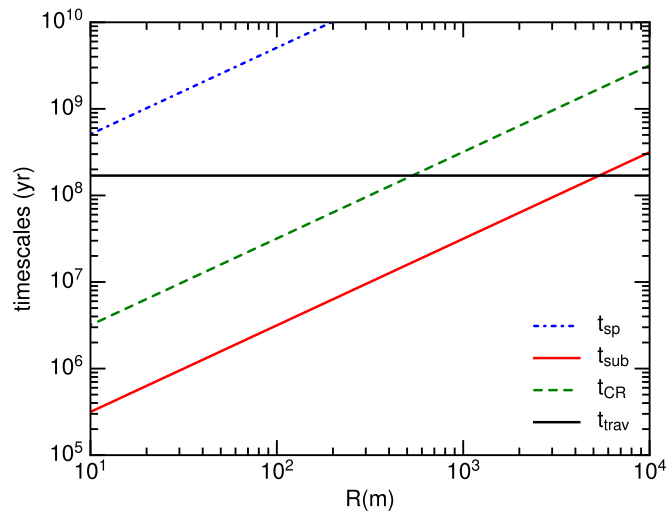

Figure 1. Comparison of various destruction timescales (slanted colored lines) as a function of the object radius (in meters) to the travel time from a GMC at a distance of 5.2 kpc, assuming a characteristic speed of 30 km s^{-1} (horizontal black line).

4.3. Destruction by Bow Shocks

For a cold GMC of temperature $T_{\rm gas} \sim 3$ K, the thermal velocity of the gas is $v_{\rm T} = (3kT_{\rm gas}/m_{\rm H})^{1/2} \sim 0.27(T_{\rm gas}/3\ {\rm K})^{1/2}$ km s^{-1}. Objects moving rapidly through the gas with $v_{\rm obj} \sim 30$ km s$^{-1} \gg v_T$, will produce a bow shock if their radius is larger than the mean free path of gas molecules (Landau & Lifshitz 1959). The mean free path for molecular collisions is $\lambda_{\rm mfp} \sim 1/(n_{\rm H}\sigma_{\rm H2}) = 10^4(10^6\ {\rm cm^{-3}}/n_{\rm H})(10^{-15}\ {\rm cm^{-2}}/\sigma_{\rm H2})$ km with $\sigma_{\rm H2}$ being the H_2 cross-section. Thus, for objects larger than $R = 10^4$ km, bow shocks are formed if the gas density $n_{\rm H} \gtrsim 10^6$ cm^{-3}. The post-shock gas has a high temperature and can be efficient in thermal sputtering. However, bow shocks are not expected to form for objects of $R < 10^4$ km and $n_{\rm H} < 10^6$ cm^{-3}.

5. Numerical Results

5.1. Destruction in the ISM

Assuming that H_2 objects of various sizes are produced in a nearby GMC, we estimate the minimum size of objects that could reach the Earth. The closest GMC, W51, is located at a distance of $D_{\rm GMC} = 5.2$ kpc. Thus, at a speed of 30 km s^{-1}, it takes $t_{\rm trav} \approx 1.6\times 10^8$ yr for objects to reach the solar system.

Figure 1 compares the various destruction times with $t_{\rm trav}$ for different object radii at a typical speed. The sublimation time is obtained using the equilibrium temperature $T_{\rm ice} = 2.9939 \approx 3$ K (see Section 2). We find that only very large objects of radius $R > 5$ km could survive thermal sublimation and reach the solar system. The minimum size of the objects that can survive is obtained by setting $t_{\rm sub} = t_{\rm trav,\ ISM}$, yielding

$$\begin{aligned} R_{\rm min,\ ISM} &= 5.4\left(\frac{D_{\rm GMC}}{5.2\ {\rm kpc}}\right)\left(\frac{30\ {\rm km\ s^{-1}}}{v_{\rm obj}}\right) \\ &\times\exp\left(100\ {\rm K}\left[\frac{1}{T_{\rm ice}} - \frac{1}{3\ {\rm K}}\right]\right){\rm km}. \end{aligned} \tag{27}$$

5.2. Destruction on the Way from the Center of GMCs to the ISM

The total gas column density toward the densest GMC amounts to extinction of $A_V \sim 200$ (see e.g., Mathis et al. 1983), which corresponds to a hydrogen column density of $N_{\rm H} \sim 3.74 \times 10^{23}\,{\rm cm}^{-2}$ based on the scaling $N_{\rm H}/A_V \approx (5.8 \times 10^{21}/R_V)\,{\rm cm}^{-2}/{\rm mag}$ with $R_V = 3.1$ (Draine 2011). Assuming a mean GMC density $n_{\rm H} = 10^4\,{\rm cm}^{-3}$ and a GMC radius $R_{\rm GMC} \approx 12$ pc, the travel time is $t_{\rm trav,GMC} = R_{\rm GMC}/v_{\rm obj}$

$$\approx 3.91 \times 10^5 (R_{\rm GMC}/12\ {\rm pc})(30\ {\rm km\ s}^{-1}/v_{\rm obj})\ {\rm yr}$$

Equation (22) implies a destruction time by gas collisions of $t_{\rm evap,gas} \sim 9 \times 10^6 (R/1\ {\rm km})(n_{\rm H}/10^4\ {\rm cm}^{-3})$ yr, which is longer than the travel time.

As shown in Section 2, collisional heating is important in GMCs because of their high density, $n_{\rm H} \gtrsim 10^3\,{\rm cm}^{-3}$. Assuming that a fraction η of the impinging proton's energy is converted into surface heating to a temperature below $T_{\rm evap}$, collisional heating raises the temperature of the surface to

$$T_{\rm ice} = \left(\frac{\eta n_{\rm H} 1.4 m_{\rm H} v_{\rm obj}^3/2}{4\sigma\epsilon_T}\right)^{1/4} \simeq 6.1\left(\frac{n_{\rm H}}{10^4\ {\rm cm}^{-3}}\right)^{1/4}\left(\frac{\eta}{\epsilon_T}\right)^{1/4}\left(\frac{v_{\rm obj}}{30\ {\rm km\ s}^{-1}}\right)^{3/4}\ {\rm K}, \quad (28)$$

which implies effective cooling by evaporation (see Equation (9)).

To find the actual equilibrium temperature, we solve Equation (12) and obtain $T_{\rm ice} \approx 3.26$ K for $n_{\rm H} = 10^4\,{\rm cm}^{-3}$, assuming $\eta = \epsilon_T = 1$. Substituting this typical temperature into Equation (3) yields

$$t_{\rm sub}(T_{\rm ice}) \simeq 2.1 \times 10^6\left(\frac{R}{1\ {\rm km}}\right) \times \exp\left(100\ {\rm K}\left[\frac{1}{T_{\rm ice}} - \frac{1}{3.26\ {\rm K}}\right]\right)\ {\rm yr}. \quad (29)$$

The minimum size of the objects that can survive is obtained by setting $t_{\rm sub} = t_{\rm trav,\ GMC}$, yielding

$$R_{\rm min,\ GMC} \approx 186\left(\frac{R_{\rm GMC}}{12\ {\rm pc}}\right)\left(\frac{30\ {\rm km\ s}^{-1}}{v_{\rm obj}}\right) \times \exp\left(100\ {\rm K}\left[\frac{1}{T_{\rm ice}} - \frac{1}{3.26\ {\rm K}}\right]\right)\ {\rm m}. \quad (30)$$

We conclude that H_2 objects cannot survive their journey from their GMC birthplace to the ISM if their radius is below $R_{\rm min,\ GMC}$. The actual value $R_{\rm min,\ GMC}$ would be larger because the surface temperature is higher when objects are moving through the core of GMCs with higher gas density.

5.3. Destruction in the Solar System

When 'Oumuamua entered the solar system, solar radiation heated the frontal surface to an equilibrium. We numerically solve Equation (12) and obtain the equilibrium temperatures $T_{\rm ice} = 7.94$ and 7.15 K at heliodistances $D = 0.25$ and 0.5 au. Substituting these temperatures into Equation (4), one obtains $t_{\rm sub} = 3.18$ and 12.72 days, assuming $R = 300$ m. These sublimation times are shorter than the travel time of $t_{\rm trav} = 0.5\ {\rm au}/v_{\rm obj} = 14.42$ days. The sputtering by the solar wind is less important than thermal sublimation.

6. Discussion

6.1. Can H_2-rich Grains form in Dense Clouds?

Seligman & Laughlin (2020) suggested that H_2 ice objects can form by means of accretion and coagulation of dust grains in the densest region of a GMC where the gas density is $n_{\rm H} \sim 10^5\,{\rm cm}^{-3}$ and temperature is $T_{\rm gas} \sim 3$ K. Below, we show that H_2-rich grains cannot form in the GMC due to destruction by collisional heating, preventing the formation of H_2 objects.

At low temperatures, the accretion of H_2 molecules from the gas phase onto a grain core is a main process enabling the formation of an H_2 mantle. The characteristic timescale for forming an icy grain of radius a is given by

$$t_{\rm acc} = \frac{m_{\rm gr}}{1.05 s_{\rm H} n_{\rm H} m_{\rm H} v_{\rm th} \pi a^2} = \frac{4\rho_{\rm ice} a}{3.15 s_{\rm H} n_{\rm H} m_{\rm H} v_{\rm th}} \simeq 10^2\left(\frac{a}{1\ \mu{\rm m}}\right)\left(\frac{n_{\rm H}}{10^5\ {\rm cm}^{-3}}\right)^{-1}\left(\frac{T_{\rm gas}}{T_{\rm CMB}}\right)^{1/2} \times \left(\frac{\rho_{\rm ice}}{0.1\ {\rm g\ cm}^{-3}}\right)\ {\rm yr}, \quad (31)$$

where the thermal velocity $v_{\rm th} = (8kT_{\rm gas}/\pi m_{\rm H})^{1/2}$, the factor 1.05 accounts for $n({\rm He})/n_{\rm H} = 0.1$, and the sticking coefficient $s_{\rm H} = 1$ is assumed.

The timescale to form H_2 ice from collisions between two icy grains of equal sizes a and relative velocity v_{gg} is given by

$$t_{\rm coag} = \frac{1}{n_{\rm gr} v_{gg} \pi a^2} = \frac{4a\rho_{\rm gr}}{3M_{d/g}\mu m_{\rm H} n_{\rm H} v_{gg} s_{\rm gr}} \simeq \frac{2.5 \times 10^5}{s_{\rm gr}}\left(\frac{a}{1\ \mu{\rm m}}\right)\left(\frac{10^5\ {\rm cm}^{-3}}{n_{\rm H}}\right) \times \left(\frac{0.1\ {\rm km\ s}^{-1}}{v_{gg}}\right)\left(\frac{0.01}{M_{d/g}}\right)\ {\rm yr}, \quad (32)$$

amounting to $\sim 10^4$ yr for a density of $n_{\rm H} \sim 10^6\,{\rm cm}^{-3}$, a sticking coefficient, $s_{\rm gr} = 1$, and the grain number density, $n_{\rm gr}$, is given by Equation (25). In conclusion, the timescale to form micron-sized grains by coagulation is much longer than the formation time by gas accretion, in agreement with the estimate by Seligman & Laughlin (2020).

However, Seligman & Laughlin (2020) did not consider the destructive effect of icy H_2 grains by collisional heating by gas. Greenberg & de Jong (1969) noted that, at a density of $n_{\rm H} > 10^5\,{\rm cm}^{-3}$, collisional heating might prevent the formation of H_2 ice. We calculate the grain temperature heated by gas with a minimum temperature $T_{\rm gas} = T_{\rm CMB} = 2.725$ K as follows:

$$T_{\rm gr} = \left(\frac{1.05 n_{\rm H} v_{\rm th} \times \pi a^2 \times 2kT_{\rm gas}}{4\pi a^2 \sigma \langle Q_{\rm abs}\rangle_T}\right)^{1/4} \simeq 3.02\left(\frac{n_{\rm H}}{10^5\ {\rm cm}^{-3}}\right)^{1/4}\left(\frac{T_{\rm gas}}{T_{\rm CMB}}\right)^{3/8}\left(\frac{10^{-4}}{\langle Q_{\rm abs}\rangle_T}\right)^{1/4}\ {\rm K}, \quad (33)$$

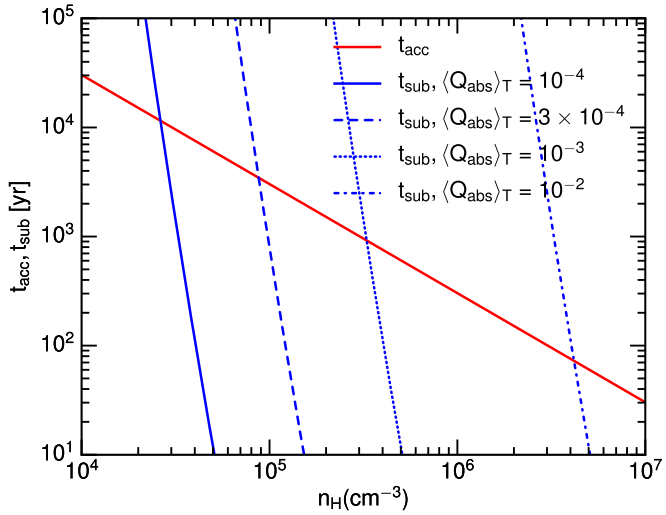

Figure 2. Comparison of accretion timescale (red line) with the sublimation time (blue lines) by collisional heating for different emissivities $\langle Q_{abs}\rangle_T$, assuming $T_{gas} = T_{CMB}$ and the grain size of $a = 1\ \mu$m. The typical emissivity at low temperatures is $\langle Q_{abs}\rangle_T = 10^{-4}$.

where $2kT_{gas}$ is the mean kinetic energy of thermal particles colliding with the grain, and $\langle Q_{abs}\rangle_T \approx 1.1 \times 10^{-4}(a/1\ \mu\text{m})(T/3\ \text{K})^2$ for silicate grains (Draine 2011). Gas collisions eventually lead to thermal equilibrium at $T_{gr} = T_{gas}$.

Substituting this typical temperature and the grain size $a = 1\ \mu$m into Equation (3) yields

$$t_{sub}(T_{gr}) \simeq 0.85\left(\frac{a}{1\ \mu\text{m}}\right)\exp\left(100\ \text{K}\left[\frac{1}{T_{gr}} - \frac{1}{T_{CMB}}\right]\right)\text{yr}, \quad (34)$$

which is much shorter than the accretion time t_{acc} given in Equation (31). The gas temperature in realistic GMCs is larger than T_{CMB} due to CR heating, resulting in a much shorter sublimation time. We therefore conclude that micron-sized H_2 grains cannot form in dense GMCs due to collisional heating.

Figure 2 shows the accretion time and sublimation time as functions of gas density for different emissivities $\langle Q_{abs}\rangle_T$. For the typical value of $\langle Q_{abs}\rangle \sim 10^{-4}$, sublimation is faster than accretion for $n_H > 2 \times 10^4\ \text{cm}^{-3}$. On the other hand, in lower density regions, accretion is faster than sublimation, but heating by CRs and interstellar radiation could still be important for heating the gas above T_{CMB} and increase sublimation of H_2 ice.

6.2. Implications: Could 'Oumuamua made of H_2 Ice Survive the Journey from the Birth Site to the Solar System?

Assuming that H_2 objects could somehow form in the densest regions of GMCs, we found that sublimation by collisional heating inside the GMC would destroy the objects before their escape into the ISM. We also studied various destruction mechanisms of H_2 ice in the ISM. In particular, we found that H_2 objects are heated by the average interstellar radiation, so that they cannot survive beyond a sublimation time of $t_{sub} \sim 10$ Myr for $R = 300$ m (see Figure 1). Only H_2 objects larger than 5 km could survive.

6.3. Implications for H_2 Ice as Baryonic Dark Matter

Primordial snowballs were suggested as baryonic dark matter (White 1996). Previous studies considered collisions between snowballs as a destructive mechanism (Hegyi & Olive 1986; Carr & Sakellariadou 1999). Hegyi & Olive (1986) studied destruction of H_2 ice by the CMB and found that at redshift $(1+z) = 3.5$, sublimation would rapidly destroy H_2 ice. Later, White (1996) argued that the treatment of sublimation by Hegyi & Olive (1986) was inadequate because evaporative cooling was not taken into account. In this work, we have shown that the evaporative cooling is only important for $T_{ice} \gtrsim 3$ K. Even when evaporative cooling is taken into account, thermal sublimation by starlight still plays an important role in the destruction of H_2 objects. The present CMB temperature T_{CMB} is not high enough to rapidly sublimate H_2 ice. However, at redshifts $z > 1$, the CMB temperatures of $T_{CMB} > 5$ K, can rapidly destroy H_2 objects of $R \sim 1$ km within $t_{sub} \sim 48$ yr, based on Equation (4).

More importantly, we found that the formation of H_2 objects cannot occur in dense GMCs because collisional heating raises the temperature of dust grains, resulting in rapid sublimation of H_2 ice mantles. Thus, we find that large objects rich in H_2 ice are unlikely to form in dense clouds, in agreement with the conclusions of Greenberg & de Jong (1969).

Lastly, if H_2 objects form via a phase transition, as proposed by Füglistaler & Pfenniger (2018), they must be larger than ~5 km to survive the journey from the GMC to the solar system.

7. Summary

We have studied the destruction of H_2 ice objects during their journey from their potential birth sites to the solar system. Our main findings are as follows.

1. Destruction of H_2 ice-rich objects by thermal sublimation due to starlight is important, whereas destruction by CRs and interstellar matter is less important.
2. The minimum radius of H_2 objects is required to be $R_{min} \sim 5$ km for survival in the ISM from the nearest GMC.
3. H_2 objects of radius $R < 200$ m could be destroyed on the way from the GMC to the ISM due to thermal sublimation induced by collisional heating.
4. Formation of H_2 ice-rich grains in dense GMCs is unlikely to occur due to rapid sublimation induced by collisional heating. This makes the formation of H_2-rich objects improbable.

We thank the anonymous referee for a constructive report, as well as Ed Turner, Ludmilla Kolokolova, Alex Lazarian, and Shu-ichiro Inutsuka for useful comments. T.H. acknowledges the support by the National Research Foundation of Korea (NRF) grants funded by the Korea government (MSIT) through the Mid-career Research Program (2019R1A2C1087045). A.L. was supported in part by a grant from the Breakthrough Prize Foundation.

ORCID iDs

Thiem Hoang https://orcid.org/0000-0003-2017-0982
Abraham Loeb https://orcid.org/0000-0003-4330-287X

References

Bacci, P., Maestripieri, M., Tesi, L., et al. 2017, MPEC, U181, 1
Bannister, M. T., Schwamb, M. E., Fraser, W. C., et al. 2017, ApJL, 851, L38
Bialy, S., & Loeb, A. 2018, ApJL, 868, L1
Carr, B. J., & Sakellariadou, M. 1999, ApJ, 516, 195
Do, A., Tucker, M. A., & Tonry, J. 2018, ApJL, 855, L10
Domokos, G., Sipos, A., Szab, G. M., & Vrkonyi, P. L. 2017, RNAAS, 1, 50
Drahus, M., Guzik, P., Waniak, W., et al. 2018, NatAs, 2, 407
Draine, B. T. 2011, Physics of the Interstellar and Intergalactic Medium (Princeton, NJ: Princeton Univ. Press)
Fitzsimmons, A., Snodgrass, C., Rozitis, B., et al. 2018, NatAs, 2, 133
Fraser, W. C., Pravec, P., Fitzsimmons, A., et al. 2018, NatAs, 2, 383
Füglistaler, A., & Pfenniger, D. 2016, A&A, 591, A100
Füglistaler, A., & Pfenniger, D. 2018, A&A, 613, A64
Gaidos, E. 2017, arXiv:1712.06721
Gaidos, E., Williams, J. P., & Kraus, A. 2017, arXiv:1711.01300
Greenberg, J. M., & de Jong, T. 1969, Natur, 224, 251
Hegyi, D. J., & Olive, K. A. 1986, ApJ, 303, 56
Hoang, T., Lazarian, A., Burkhart, B., & Loeb, A. 2017, ApJ, 837, 5
Hoang, T., Lazarian, A., & Schlickeiser, R. 2015, ApJ, 806, 255
Hoang, T., Loeb, A., Lazarian, A., & Cho, J. 2018, ApJ, 860, 42
Jewitt, D., Luu, J., Rajagopal, J., et al. 2017, ApJL, 850, L36
Landau, L. D., & Lifshitz, E. M. 1959, Fluid Mechanics, Teoreticheskaia Fizika (Oxford: Pergamon Press)
Leger, A., Jura, M., & Omont, A. 1985, A&A, 144, 147
Mashchenko, S. 2019, MNRAS, 489, 3003
Mathis, J. S., Mezger, P. G., & Panagia, N. 1983, A&A, 128, 212
Meech, K. J., Weryk, R., & Micheli, M. e. a. 2017, Natur, 552, 378
Micheli, M., Farnocchia, D., Meech, K. J., et al. 2018, Natur, 559, 223
Moro-Martin, A. 2019, ApJL, 872, L32
Rafikov, R. R. 2018, ApJL, 867, L17
Raymond, S. N., Armitage, P. J., & Veras, D. 2018, ApJL, 856, L7
Rice, M., & Laughlin, G. 2019, ApJL, 884, L22
Sandford, S. A., & Allamandola, L. J. 1993, ApJ, 409, L65
Sekanina, Z. 2019, arXiv:1905.00935
Seligman, D., & Laughlin, G. 2020, ApJL, 896, L8
Sugiura, K., Kobayashi, H., & Inutsuka, S.-i. 2019, Icar, 328, 14
Trilling, D. E., Mommert, M., Hora, J. L., et al. 2018, AJ, 156, 261
Watson, W. D., & Salpeter, E. E. 1972, ApJ, 174, 321
White, R. S. 1996, Ap&SS, 240, 75
Zhang, Y., & Lin, D. N. C. 2020, NatAs, in press (doi:10.1038/s41550-020-1065-8)